

# Fiber Positioning Accuracy from Fiber Dithering

– March 2020

## DESI-5572

Edward F. Schlafly  
LLNL

March 18, 2020

## 1 Introduction

The Dark Energy Spectroscopic Instrument relies on the ability to quickly and accurately position fibers in the focal plane such that light from targeted stars and galaxies can be collected in the spectrographs. DESI-579 specifies that the focal plane system shall place the fiber tips within 10  $\mu\text{m}$  RMS of their nominal target positions (IN.FPA.2003) and that each tip will be placed within 35  $\mu\text{m}$  absolute of its nominal target position (IN.FPA.2004). This document focuses on the first of those two requirements. The dither analysis adopted here to address the first requirement is susceptible to occasional large outliers, due to, for example, nearby blended stars, making this analysis inappropriate to addressing that requirement.

We assess the accuracy of the fiber positioning by taking a sequence of exposures of the same set of objects, with fibers intentionally dithered somewhat off of their target locations in a random pattern. By taking 12 of these exposures, we can essentially centroid the light coming down the fibers over the 12 exposures to precisely locate the light in the focal plane. The difference between these light centroids and the nominal locations in which we would have placed fibers gives the fiber positioning errors.

Accurate centroiding of each target requires care. The point-spread function of the system may vary significantly from exposure to exposure, so not all variation in light entering a fiber stems from the fiber offsets and dithers. The transparency of the night sky may also vary from exposure to exposure, and the overall telescope pointing can shift over the sequence. We solve for all of these nuisance parameters simultaneously with the fiber positioning errors of each fiber to derive the fiber positioning accuracy.

The dither analysis is most sensitive to the accuracy with which positions as measured in the Fiber View Camera (FVC) images can be used to predict positions on the sky. Any error in that transformation will result in a fixed

systematic throughout the dither sequence. Random errors in individual positioner moves or FVC centroid locations will contribute noise to the dither analysis, but will be averaged down somewhat over the 12 dither exposures. Other analyses have indicated that positioners can be placed at a particular FVC pixel with an RMS of  $10\ \mu\text{m}$ , in line with requirements. That leaves the FVC-to-sky transformation as the remaining potential factor limiting system performance.

This document uses a plate scale of  $70\ \mu\text{m}/\text{arcsec}$  to convert from arcseconds (as measured in the dither analysis) to  $\mu\text{m}$  in the focal plane. The plate scale varies from  $67.4\ \mu\text{m}/\text{arcsec}$  in the center of the field of view to  $74\ \mu\text{m}/\text{arcsec}$  on the edge; weighted by area, the mean plate scale is  $70.7\ \mu\text{m}/\text{arcsec}$ , not far from the value we have adopted.

## 2 Current Status

Figure 1 shows our best measurement of the current errors in the fiber positioning. The RMS is  $11\ \mu\text{m}$ , combining the  $x$  and  $y$  uncertainties. This is very close to the  $10\ \mu\text{m}$  requirement (IN.FPA.2003).

The distribution of positioning errors is shown in Figure 2. They have a high-order distribution with more power in the radial direction than the azimuthal. This suggests slight remaining errors in the modeling of the FVC-to-sky transformation. Updates to the dither analysis better incorporating FVC-predicted positioner offsets may improve the measurement of these remaining errors.

## 3 Improvements in Fiber Positioning

Fiber positioning accuracy has been steadily improving. At the beginning of the year, the dither analysis showed that the fibers were dramatically offset ( $10''$  RMS) from their targets with a rotational pattern. A software bug was discovered that led the hexapod to be rotated by  $\sim 400''$  relative to the needed rotation to put fibers on target. On January 23 this issue was resolved, and positioning accuracy improved to  $70\ \mu\text{m}$  ( $\sim 1''$ ) RMS positioning error, as measured by dither analyses. The FVC lens was then replaced with a lens with lower distortion, and following February 8 fiber positioning accuracy reached  $30\ \mu\text{m}$  RMS. Dither analysis results were then incorporated into PlateMaker on March 6 to account for residual effects, leading to the current  $11\ \mu\text{m}$  RMS accuracy.

## 4 Fiber Positioning with Elevation

The Level 3 requirement L3.3.2 specifies that DESI shall meet all of its requirements while at observing with zenith angles between 0 and 60 degrees. Dither sequences taken at a variety of zenith angles show that our fiber positioning

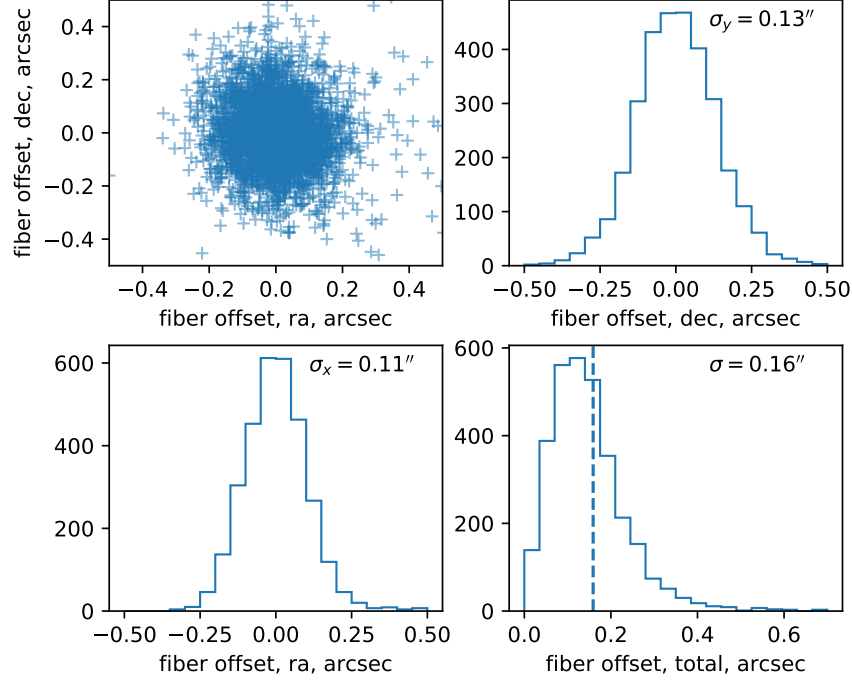


Figure 1: Fiber positioning errors for a sequence of exposures with dithered fiber positions taken  $9^\circ$  from zenith. The four panels show the distribution of fiber positioner errors in 2D, and in  $y$ ,  $x$ , and overall offset individually. The lower right panel shows our final result of  $0.16''$  overall positioning RMS.

performance is largely insensitive to zenith angle. Figure 3 shows the fiber positioning offsets obtained for a field at a zenith distance of  $54^\circ$ . Fiber positioning errors have an RMS of  $13 \mu\text{m}$ , comparable to the performance at zenith of  $11 \mu\text{m}$  obtained near zenith. The high airmass field available had significantly lower stellar density than the zenith field, leading to fewer available bright stars and greater uncertainties in the dither analysis; we expect that most of the excess noise in the high-airmass field owes to uncertainty in the dither analysis rather than differing fiber positioning accuracy.

Additional dither sequences are necessary to measure the residual fiber positioner offset pattern with higher fidelity and to test its variability with hour angle and declination. If the residual pattern is found to be fixed in time, it would be conceptually straightforward to incorporate it into the PlateMaker modeling.

## 5 Chromatic Performance

Analysis of the fiber positioning offsets at different wavelengths shows that the ADC is working as expected. Figure 4 compares fiber offsets at  $B$  wavelengths as compared with those at  $Z$  wavelengths; nonzero arrows indicate that the light centroids in the focal plane at different wavelengths are offset from one another. Vectors point from the  $Z$  centroid to the  $B$  centroid. The Figure shows the results of a dither analysis for a sequence of exposures taken at a zenith distance of  $9^\circ$ . The left panel shows the dither analysis, as compared with a ray-tracing analysis of the optics in the middle panel, and a ray-tracing analysis of the optics with the ADCs zeroed (right panel). The ray-tracing analysis is described in DESI-5556. The left and middle panels show good agreement, validating the chromatic performance of the optical system. Comparison with the right panel shows that the ADC is working correctly; the predicted large differential chromatic refraction over the field in the right panel, corresponding to zeroed ADCs, is removed in the left and middle panels, where the ADCs have been correctly set for the field.

Figure 5 shows a similar plot to Figure 4, but for a field at a zenith distance of  $54^\circ$ , just within the range of the ADC. The observed centroid differences (left) well match the ray-tracing predictions (center). Absent an ADC, typical  $B - Z$  offsets would be  $> 1''$  for this sequence (right).

## 6 Conclusion

Dither analysis shows that as of March 6, fiber positioning accuracy of  $11\ \mu\text{m}$  is obtainable. Even at a zenith distance of  $54^\circ$ , we measure a positioner accuracy only slightly worse,  $13\ \mu\text{m}$ , and expect that much of the additional noise comes from statistical uncertainty in the dither analysis. The performance of the ADC is nominal, and the variations in light centroid with wavelength are as expected from the optical design and a ray-tracing analysis. Additional dither sequences must be observed to place tighter limits on the current fiber positioning accuracy and to test the variability of the currently observed positioning errors.

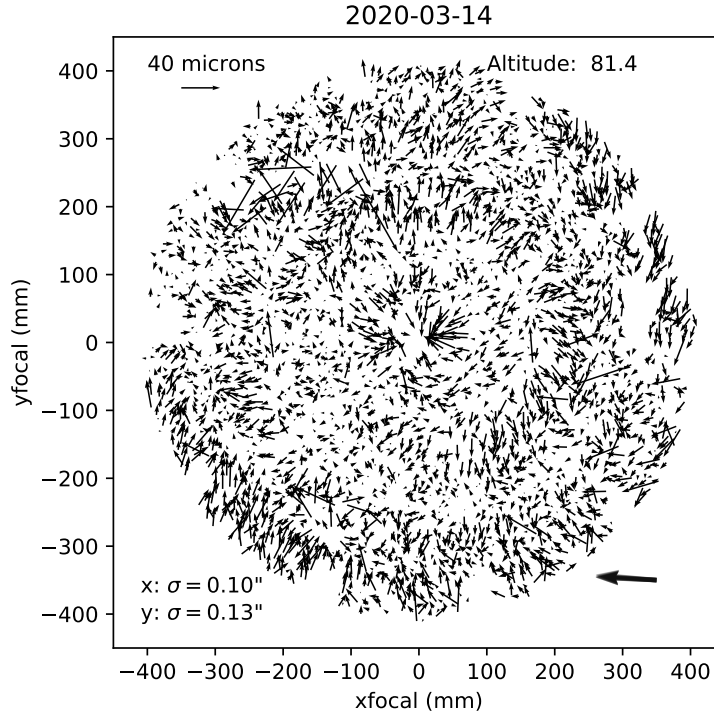


Figure 2: Fiber positioning errors for a sequence of exposures with dithered fiber positions taken  $9^\circ$  from zenith. Arrows point from the true star centers to the locations at which PlateMaker would have positioned the fibers. A  $40\ \mu\text{m}$  scale bar is provided in the upper left for comparison. The direction to zenith is given in the lower right. The current fiber positioning leaves errors of about  $0.16''$  in scale, with a high-frequency, predominantly radial error pattern suggestive of residual errors in the FVC-sky transformation.

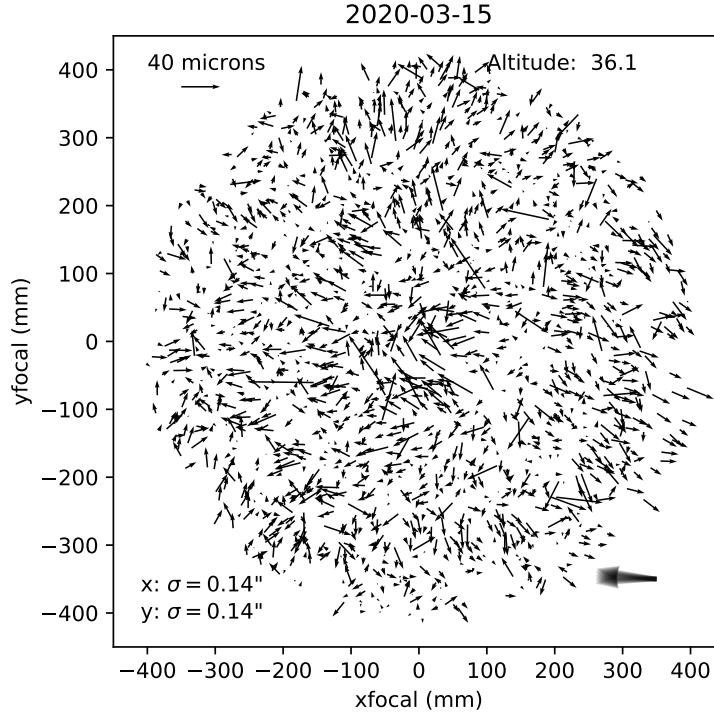


Figure 3: Fiber positioning errors for a sequence of exposures taken at a zenith distance of  $54^\circ$ . The RMS of  $13 \mu\text{m}$  is very close to the high-altitude performance of  $11 \mu\text{m}$ . The larger salt-and-pepper noise suggests that the analysis is limited by the larger statistical uncertainty on this field as compared with the high altitude field, owing to the lower stellar densities and therefore fainter typical stars present on this field.

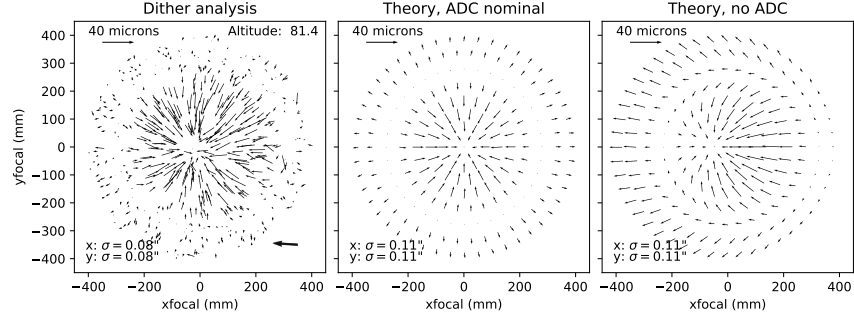


Figure 4: Difference in locations of light centroids in the focal plane at different wavelengths (left). Vectors are shown going from the  $Z$  band centroid to the  $B$  band centroid. This field, observed at a zenith distance of  $9^\circ$ , has been well corrected for atmospheric chromatic differential refraction. There is essentially no mean shift between light of different wavelengths. The offsets show the same radial pattern expected from a ray-tracing analysis of the optics (middle). Were the ADCs set at zero rather than correctly set for this field, a ray-tracing analysis predicts a small shift in field center between  $B$  and  $Z$  in the direction of the parallactic angle (right panel).

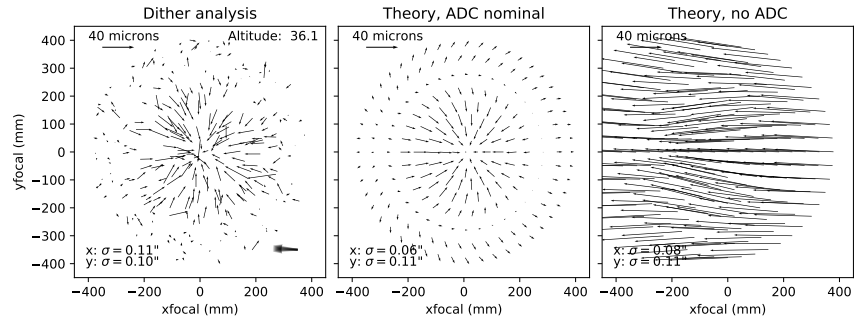


Figure 5: Difference in locations of light centroids in the focal plane at different wavelengths, as in Figure 4. This field, however, is at a zenith distance of  $54^\circ$ . Even at this high airmass, the observed centroid differences (left) are consistent with the predictions from ray tracing (center). Absent an ADC, a large,  $> 1''$  constant offset between the different bands would be present (right).